ENERGY TRANSFER MECHANISMS IN WHITE OLEDS

Luke Kelly (s4699025)

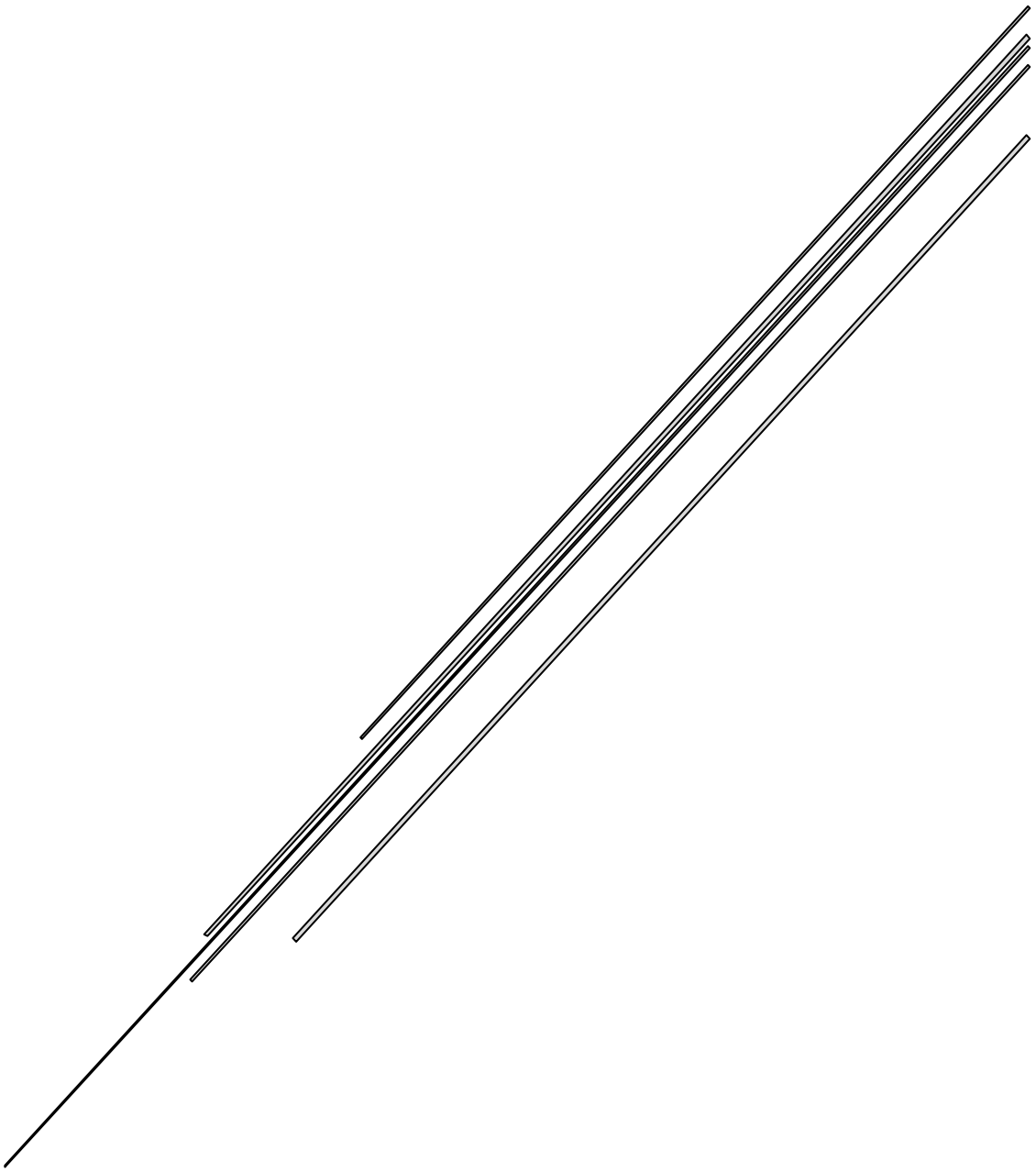

School of Chemistry and Biomolecular Sciences (COPE)

SCIE3260

Abstract

Energy transfer between multiple phosphorescent emitters and a host plays a key role in the emissive blend of white OLEDs. In this work, red and blue phosphorescent emitters in a TCTA host were investigated to characterise the energy transfer process using broadband time-resolved photoluminescence measurements. Several blend ratios were investigated, with a varying amount of red emitter and a fixed amount of blue emitter, with their energy transfer rates measured. The measured energy transfer rates were dependent on the separation distance between a red and blue emitter, consistent with Förster energy transfer. This evidence provides insight in understanding white OLEDs and efficient optimisation of blend ratios within emissive layers of white OLED devices.

Introduction

White organic light emitting diodes (OLEDs) are important for lighting applications and backlights for displays. One of the simplest ways to make a white OLED is to combine multiple different coloured narrowband emitters in a single emissive layer. Energy transfer will occur between emitters of differing energy where the energy will cascade from higher to lower energy emitters. Typically, a combination of red, green, and blue emitters is used within a white OLED. Blue emitters are higher in energy compared to green and red emitters. As such, blue emitters can transfer energy to the green and red emitters. [1][2] Phosphorescent emitters are typically used in OLED devices, so the nature of energy transfer between emitters may be Förster, Dexter or a combination of both. However, there is debate within the literature as to which mechanism dominates. This investigation aims to characterise the energy transfer mechanism of a blend of blue ('MKK-04-12') and red ('MKK-02-69') emitters with a TCTA host.

At present, emitter blends within white OLEDs are optimised through trial and error. Further understanding of energy transfer properties could be of use in predicting optimal ratios of emitters within white blends. There is also rising interest in understanding the distribution of emitters within OLED layers. This has been assumed to be random and uniformly dispersed, however, there is evidence to suggest this may not be the case [3]. Energy transfer processes between emitters are extremely sensitive to distance and are ideal in probing the separation between emitters. Therefore, investigation of the energy transfer processes in white OLEDs may reveal further evidence of aggregation between emitters.

There are two energy transfer processes. The first, Dexter energy transfer is a short-range (~1 nm) electron transfer process with an exponential dependence on the separation distance between two emitters [4], which can be expressed as

$$k_{ET} \propto J e^{-\frac{2r}{L}}, \quad (1)$$

where k_{ET} is the energy transfer rate, r is the donor-acceptor separation distance, J is the spectral overlap integral, and L is the sum of the Van der Waals radii of the two emitters.

The second mechanism is Förster energy transfer, a long-range (several nm) dipole coupling interaction that is very sensitive to the donor acceptor separation distance. The rate of Förster energy transfer is given by

$$k_{ET} = \frac{1}{\tau_D}\left(\frac{R_0}{r}\right)^6, \quad (2)$$

where τ_D is the donor lifetime and R_0 is the Förster radius [5]. The spectral overlap integral term, J, can be calculated from the donor photoluminescent (PL) emission spectrum, $P_D(\lambda)$, and the molar extinction coefficient spectrum, $\epsilon_A(\lambda)$, of the acceptor, where λ is wavelength.

$$J = \int P_D(\lambda)\epsilon_A(\lambda)\lambda^4 d\lambda. \quad (3)$$

Five blend ratios were investigated through varying the red to blue emitter ratio by weight, with the amount of blue emitter in the blend fixed at 20 wt%. The amount of red emitter investigated were 0.2, 0.4, 0.8, 1.6 and 3.2 wt%, with the remaining mass percentage being TCTA. Each blend was dissolved in toluene before spin-coating onto fused silica substrates. Time resolved photoluminescence (TRPL) was performed with each sample under vacuum with excitation at 355 nm with a pulsed laser.

Results and Discussion

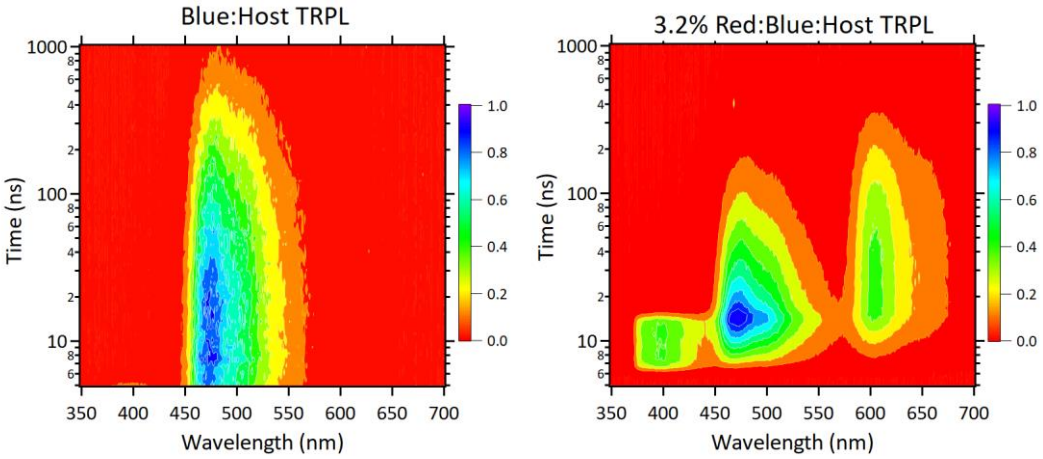

Figure 1: (a) Blue:Host 'neat' film TRPL contour plot (b) 3.2% Red blend film TRPL contour plot

The time and spectrally resolved photoluminescence decays of the blend containing 20 wt% blue emitter (a) and 20 wt% blue and 3.2 wt% red emitters (b) are shown in Figure 1. Comparing the blue-only sample and the sample containing blue with 3.2 wt% red, showed that the decay of the PL from the blue emitter was faster in the presence of the red emitter. This suggests that the addition of the red emitter introduces an additional decay rate to the blue emitter, namely energy transfer. This increase in blue PL decay can be seen more clearly in comparing the PL intensity decay of the blue emitter with increasing red emitter concentration, which shows an increase in the decay rate with increasing concentration (see Figure 2a). To extract the energy transfer rate from the PL decay data the following approach was used.

The PL intensity of the blends can be represented by respective exponential decay equations.

$$I_{Blue}(t) = I_0 e^{-(k_R + k_{NR})t}, \quad (4)$$

$$I_{Blend}(t) = I_0 e^{-(k_R + k_{NR} + k_{ET})t}. \quad (5)$$

Equation 4 represents the intensity of the blue emitter over time, t, with initial (peak) intensity I_0, radiative decay rate k_R and non-radiative decay rate k_{NR}. Equation 5 represents a similar function for the intensity of an emissive blend (blue and red emitters) with the inclusion of the energy transfer decay rate k_{ET}. Isolating a function dependent on only the energy transfer decay rate can be done by dividing Equation 5 by Equation 4 [5]

$$I_{ET}(t) = \frac{I_{Blend}(t)}{I_{Blue}(t)} = \frac{I_0 e^{-(k_R + k_{NR})t}}{I_0 e^{-(k_R + k_{NR} + k_{ET})t}} = e^{-(k_{ET})t}. \quad (6)$$

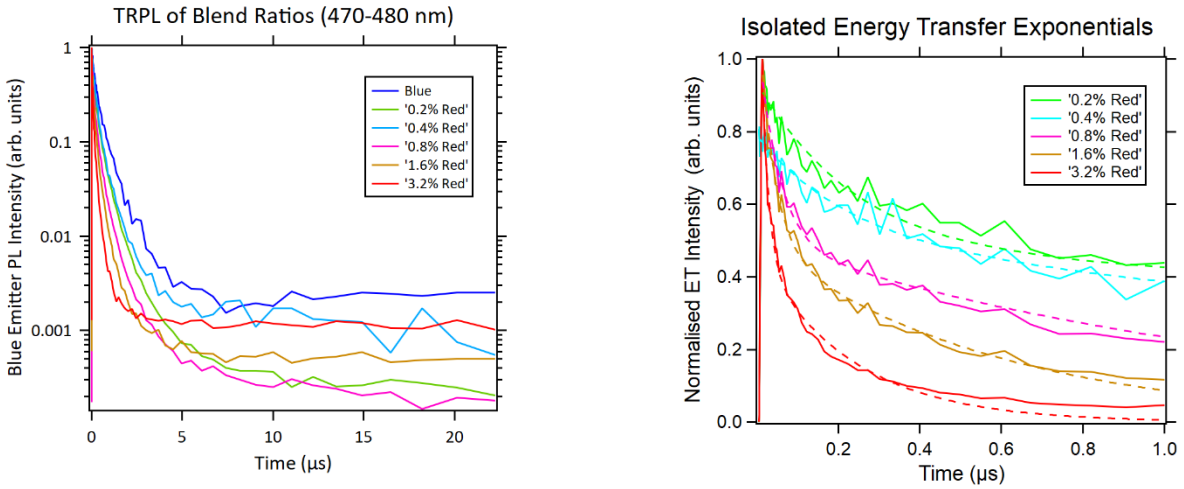

Figure 2: (a) Comparison of PL intensity for each blend ratio (b) Extraction of energy transfer decay for each blend ratio.

Applying Equation 6 to the TRPL data collected for the blue sample ($I_{Blue}(t)$) and each blend ($I_{Blend}(t)$), Figure 2b can be plotted, which is essentially the energy transfer component of the PL decay, i.e., normalised I_{ET} (log scale) against time. The decay curves could be fitted with a double exponential fit using Igor Pro 8. The lifetimes obtained from the fits (τ_1 and τ_2) were converted to decay rates and averaged, weighted by the amplitude of each exponential term (A_1 and A_2)

$$I_{k_{ET}}(t) = y_0 + A_1 \exp\left(\frac{-(t-t_0)}{\tau_1}\right) + A_2 \exp\left(\frac{-(t-t_0)}{\tau_2}\right). \quad (7)$$

The average energy transfer rates for each red emitter concentration are summarised in Table 1.

Table 1: Values of energy transfer decay fitments and average energy transfer rates.

Sample (Red %)	A_1	τ_1^{-1} ($\times 10^7\ s^{-1}$)	A_2	τ_2^{-1} ($\times 10^7\ s^{-1}$)	Average Rate ($\times 10^7\ s^{-1}$)
0.2	0.44 ± 0.02	0.44 ± 0.05	0.48 ± 0.02	0.12 ± 0.01	0.22 ± 0.03
0.4	0.27 ± 0.05	0.4 ± 0.1	0.51 ± 0.05	0.29 ± 0.09	0.18 ± 0.05
0.8	0.44 ± 0.02	2.0 ± 0.2	0.49 ± 0.02	0.76 ± 0.06	1.0 ± 0.1
1.6	0.47 ± 0.02	2.7 ± 0.2	0.49 ± 0.02	1.8 ± 0.1	1.4 ± 0.1
3.2	0.53 ± 0.02	6.0 ± 0.6	0.44 0.02	4.4 0.3	3.5 ± 0.4

Values in Table 1 were determined through a double exponential fit (Equation 7). Considering Equation 6, ideally a single exponential model would fit most accurately. A double exponential fit being more accurate indicates there are other variables that impact the energy transfer rate. With an excess of blue emitters in a film, there a range of separation distances between any red emitter and a blue emitter. In turn, this would produce a range of decay rates due to energy transfer within the film and may be one cause of a double exponential model being a more accurate fit to the data than a single. However, the sensitivity of the Förster mechanism would suggest that the emitters closest to the Förster radius would dominate in terms of the energy

transfer decay rate. Therefore, a weighted average of the two fitted rates is a reasonable approximation for the determination of the energy transfer rate.

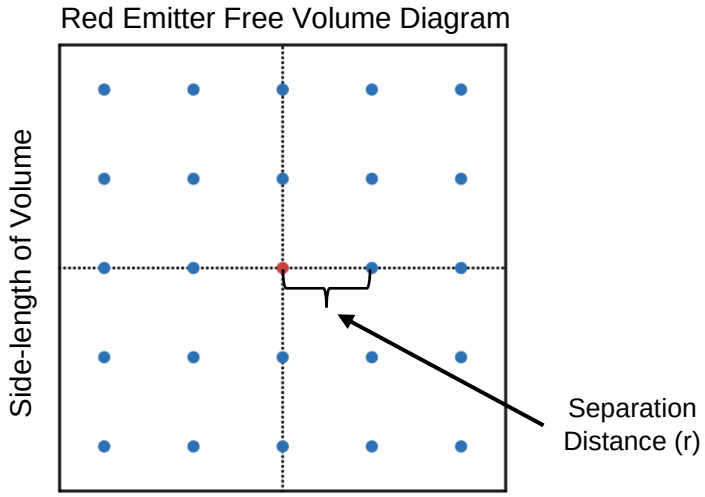

Figure 3: Separation distance between donors and acceptor diagram.

To investigate the mechanism of energy transfer between the emitters, the separation distance between emitters, r, needs to be estimated (see Figure 3Figure 3, note that while the diagram shows a two-dimensional representation, the calculation was performed in three-dimensional space). Taking a simple approach, assuming all the emitters are equally distributed in space, the total free volume per red emitter was first calculated. With this, the total number of emitters within a 'red volume' was calculated. Modelling the free space per red emitter as a cube, the side length of the volume per emitter (red and blue) was calculated and said to be the average separation distance between any red and blue emitter pair.

Table 2: Estimated separation distances between blue and red emitters (4 sigfig).

Sample (Red %)	**0.2**	**0.4**	**0.8**	**1.6**	**3.2**
Modelled Sep. Distance (nm)	2.405	2.399	2.388	2.365	2.323

To fit the energy transfer rate data against separation distance with respect to both Dexter and Förster mechanisms, the spectral overlap integral term J and the donor lifetime τ_D needs to be calculated, respectively. The spectral overlap term is calculated from solution-based measurements of donor PL emission and acceptor molar extinction coefficient, seen in Figure 4. Taking the integral of the overlapping integral allows for the value of J to be calculated. Fitting k_{ET} against separation distance r with a singular exponential model with the value J fixed, a poor exponential fit is achieved, with non-physical parameters, and the data is not consistent with Dexter energy transfer (see Figure 5a).

Using the same method to determine the values within Table 1, the data for the blue-only sample (Figure 2b) was used to determine the average lifetime of the blue chromophore as 0.23 ± 0.05 µs. Linearising the separation distance to fit the Förster model, a linear model is applied to k_{ET} against r, seen in Figure 5b. A good fit is achieved and indicates that the data is consistent with Förster energy transfer. Moreover, this is consistent with previous studies on energy transfer in phosphorescent emitters [6].

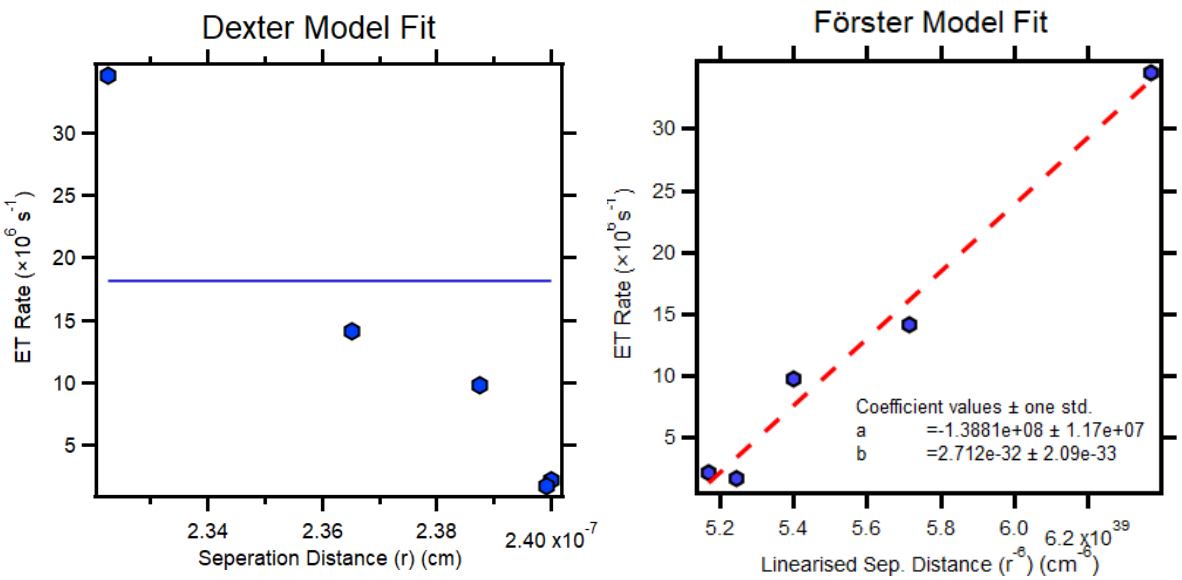

Figure 4: (a) Dexter energy transfer model fit (b) Förster energy transfer model fit.

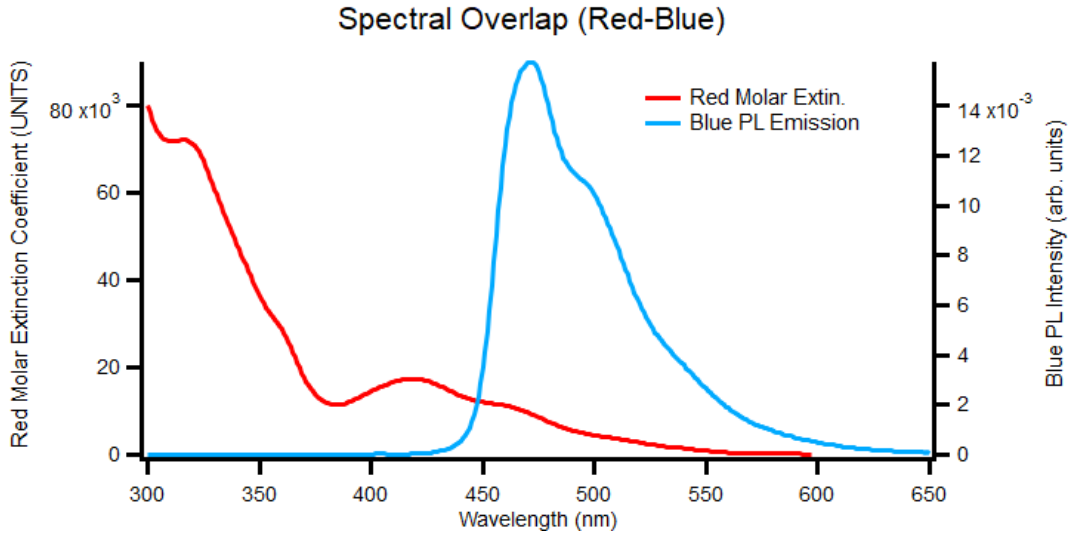

Figure 5: Donor PL emission and acceptor molar extinction coefficient overlap.

Using the gradient obtained from the fit to the data in Figure 44b, and the measured blue lifetime, τ_D, the Förster radius R_0 for the solid-state films was calculated to be 4.3 ± 0.2 nm. Using solution-based measurements (Figure 5), the spectral overlap integral term for the emitters in solution was calculated and a Förster radius of 3.8 nm was calculated for energy transfer between the blue and red emitter. The use of average lifetimes and energy rates represents a significant simplification analysis. Further improvements could be made with additional exponential terms to fully describe the PL decay data. Furthermore, energy transfer between blue emitters can occur through the Förster mechanism as the spectral overlap between the blue PL and extinction coefficient spectrum is non-zero. Following the same calculation taken from Figure 5, the Förster radius between two blue emitters is 1.3 nm. Being much shorter in comparison to the respective red-blue Förster radius, the energy transfer between blue emitters is much less prominent. However, it should be accounted for in future work as the transfer of excitation between the blue emitters will increase the probability of encountering a red emitter.

An increased Förster radius observed in solid state blends indicates that the energy transfer rate is greater than expected from the solution-based measurements. This increase in energy transfer rate suggests that the emitters may be closer together (aggregated) than they would be if they were dispersed uniformly. The method of modelling the separation distance between the emitters used (see Figure 3) is very approximate and has been used to determine the energy transfer process. This is a source of inaccuracy within the approach and may impact the calculated Förster radius for the samples. To increase the validity of the separation distance values, and hence evidence of aggregation, molecular dynamics simulations can be used to model the morphology of the emitters [3].

Conclusion

In summary, thin films of red, blue and host emitter blends were prepared at varying ratios of red emitter by weight to characterise the energy transfer process between the blue and red emitters. Time resolved photoluminescence of each blend revealed that increasing the red emitter concentration within the film resulted in an increase in the energy transfer rate. Furthermore, by estimating the average separation distance between red and blue emitters in each concentration it was found that the energy transfer process was consistent with Förster energy transfer and not Dexter energy transfer. The solid state Förster radius between red-blue emitter pairs was determined as 4.3 ± 0.2 nm, while solution based Förster radii for blue-blue and red-blue emitter pairs were determined as 1.3 nm and 3.8 nm respectively. These results are in good agreement despite several assumptions and simplifications in the analysis. Further work should focus on improving separation distance modelling, perhaps through molecular dynamics simulations [3]. Moreover, the donor lifetime determination can be improved through accounting for additional decay rates, namely Förster energy transfer between blue emitters. Investigation of a three-emitter blend, introducing green, would develop a clearer understanding of energy transfer within a typical white OLED.

Experimental Section

Sample preparation: Solution based blends prepared by weight percentages in toluene with a fixed 20 wt% of blue emitter in each blend; 0, 0.2, 0.4, 0.8, 1.6 and 3.2 wt% red, with the remainder of the blend consisting of the host TCTA. Each blend solution was prepared using stock solutions of each component; 7.5 mg/ml for blue and TCTA, 0.075 mg/ml for red (in toluene). The solutions were spin-coated onto fused silica substrates and stored under vacuum before and after taking measurements.

Time-resolved PL measurements: TRPL performed using an ‘OPOTEK Opolette 355 LD tuneable laser’ at 355 nm passing through a band pass filter, incident on each sample, secured in a vacuum chamber at 300K. PL emission captured through a long pass filter by an ‘Andor KYMERA – Adaptive image focusing spectrograph’ and processed by an ‘ANDOR IStar ICCD’. ‘Andor SOLIS for spectroscopy’ software used for data acquisition of TRPL. A continuous spectrum acquisition was taken of each sample before a kinetic acquisition and afterwards. Kinetic acquisitions were taken using a digital delay gate (DDG) set logarithmically with a delay width set to 4 ns. Data processed using Igor Pro 8 64-Bit after zeroing the background intensity of collected data and normalising on Excel.

Acknowledgments and References

In writing this report, for help with sample preparation, equipment training, and supervision, I would like to acknowledge:

Sampath Ranasinghe, Isaac Etchells, Manikandan Koodalingam, Paul Burn and Paul Shaw (Supervisor).

[1] D'Andrade, B. W.; Forrest, S. R. White Organic Light-Emitting Devices for Solid-State Lighting. *Advanced Materials* **2004**, *16* (18), 1585–1595.

[2] Reineke, S.; Thomschke, M.; Lüssem, B.; Leo, K. White Organic Light-Emitting Diodes: Status and Perspective. *Reviews of Modern Physics* **2013**, *85* (3), 1245–1293.

[3] Gao, M.; Lee, T.; Burn, P. L.; Mark, A. E.; Pivrikas, A.; Shaw, P. E. Revealing the Interplay between Charge Transport, Luminescence Efficiency, and Morphology in Organic Light-Emitting Diode Blends. Advanced Functional Materials 2019, 30 (9), 1907942.

[4] Murphy, C. B.; Zhang, Y.; Troxler, T.; Ferry, V.; Martin, J. J.; Jones, W. E. Probing Förster and Dexter Energy-Transfer Mechanisms in Fluorescent Conjugated Polymer Chemosensors. *The Journal of Physical Chemistry B* **2004**, *108* (5), 1537–1543.

[5] Lakowicz, J. R. *Principles of Fluorescence Spectroscopy*; Springer: New York, New York, 2016.

[6] Kawamura, Y.; Brooks, J.; Brown, J. J.; Sasabe, H.; Adachi, C. Intermolecular Interaction and a Concentration-Quenching Mechanism of Phosphorescent Ir(Iii) Complexes in a Solid Film. *Physical Review Letters* **2006**, *96* (1).

[7] Lee, T.; Sanzogni, A. V.; Burn, P. L.; Mark, A. E. Evolution and Morphology of Thin Films Formed by Solvent Evaporation: An Organic Semiconductor Case Study. *ACS Applied Materials & Interfaces* **2020**, *12* (36), 40548–40557.

[8] Ruseckas, A.; Shaw, P. E.; Samuel, I. D. Probing the Nanoscale Phase Separation in Binary Photovoltaic Blends of Poly(3-Hexylthiophene) and Methanofullerene by Energy Transfer. *Dalton Transactions* **2009**, No. 45.

[9] Saghaei, J.; Koodalingam, M.; Burn, P. L.; Pivrikas, A.; Shaw, P. E. Light-Emitting Dendrimer:Exciplex Host-Based Solution-Processed White Organic Light- Emitting Diodes. *Organic Electronics* **2022**, *100*.